REVIEW

A Review of Research on Galvanic Corrosion of Aluminum Alloys

Huixin Zhu, Mingzhe Leng[*], Guofeng Jin[*] and Heyang Miao

Xi'an Institute of High Technology, Xi'an, 710038, China

[*]Corresponding Authors: Mingzhe Leng. Email: lmz_198810@163.com; Guofeng Jin. Email: douhao616@126.com

ABSTRACT

When aluminum alloys are coupled with dissimilar materials, they often act as corrosion anodes and are suscepted to accelerated corrosion. Therefore, deepening our knowledge of such corrosion phenomena, related mechanisms, and elaborating new prediction model is of great theoretical and practical significance. In this paper, such mechanisms are explained from both macroscopic and microscopic points of view by considering several aspects such as the second phase particle type, grain size, and environmental ions. More specifically, different perspectives on such a problem are elaborated, which take into account: the properties of the coupling pair materials, geometrical characteristics, environmental media characteristics, the corrosion regularity of different types of aluminum alloys, the influence of area ratio on anode corrosion current density, the interference of the solution primary ions represented by Cl- and the accompanying ions represented by Al^{3+}. A review is also conducted of the standard test methods used in the study of aluminum alloys galvanic corrosion and of research methods such as the Wire Beam Electrodes Technology (WBE), the Scanning Kelvin Probe Force Microscopy (SKPFM) technology. Finally, three kinds of inhibition technologies are discussed, including the anodic oxidation treatment, the corrosion inhibitor treatment and the coating protection method.

KEYWORDS

Aluminum alloy; microgalvanic corrosion; influencing factors; first principles calculations

1 Introduction

Galvanic corrosion refers to a phenomenon in which two different metals in the same corrosive medium come into contacting with each other, resulting in the formation of galvanic cells driven by corrosion potential difference, thus intensifying the corrosion tendency of relatively inert low metals [1]. In production and life, galvanic corrosion is very common. For example, the famous corrosion history of 'Statue of Liberty' reported by Jonathan [2] showed that the copper outer layer of the Statue with high corrosion potential was in close contact with the inner steel bracket with low corrosion potential, and the electrolyte environment provided by water. The coupling of the two caused a serious galvanic corrosion, which led to the corrosion of nearly half of the steel supports. Compared with steel and other materials, aluminum alloy has been widely used in various fields in recent decades due to its advantages of high strength, low density, and excellent machining performance. Although an aluminum alloy surface is easy to develop passivation film, due to the multifarious upgrading steps of the industrial chain and long replacement cycle of large equipment, it is often easy to form galvanic corrosion with dissimilar metals [3]. Aluminum alloy has a low electrical coupling sequence (approximately −0.78 to −1.02 V in seawater

flowing at 25°C [4,5]), and is more inclined to be subjected to accelerated corrosion as an anode when coupled with most dissimilar metals like stainless steel [6]. When the galvanic corrosion progresses to a certain extent, it can lead to aluminum alloy storage tanks developing invisible or even overt corrosion holes and cracks, running, bubble, drip, leakage, and other accidents; At the same time, corrosion products will also pollute propellant, oil and other fuels, affecting the safety and reliability of fuel combustion [7]. In the actual processing and application of aluminum alloys, the material modification problem caused by micro-galvanic corrosion of aluminum alloy also needs to be solved urgently. For example, the friction stir welding (FSW) process of aluminum alloy can greatly avoid the hot crack sensitivity caused by traditional welding, and effectively promote the manufacturing of complex aluminum alloy components [8]. However, in practice, FSW will produce strongly modified structures that are completely different from the base metal, resulting in the friction stir welded joint and its adjacent areas showing stronger galvanic corrosion sensitivity under stress conditions [9–13]. Therefore, the study of galvanic corrosion of aluminum alloy has very importantly theoretical and practical significance.

It is worth noting that the macroscopic galvanic corrosion emphasizes the accelerated corrosion of anode materials formed after the coupling of materials with different properties, while the microscopic galvanic corrosion emphasizes the galvanic corrosion between different microscopic particles after the three conditions of galvanic corrosion (potential difference, electronic conductive branch, and ion conductive branch) are met on the surface of the same material. However, whether macroscopically or microscopically, it is the main direction in the study of galvanic corrosion of aluminum alloy to explore the role of microstructure in galvanic corrosion. Studies have shown that the second phase particles represented by Al_7Cu_2Fe and Al_2Cu have a positive volt potential relative to the aluminum matrix. On the contrary, Al_2CuMg and Mg_2Si have negative potentials [14], and these primary particles are often important areas for the initiation and derivation of galvanic corrosion after coupling with aluminum matrix. Campestrini et al. [15] and Andreatta et al. [16] revealed that heat treatment can change the electrochemical reactivity of particles, thus affecting the corrosion sensitivity of aluminum alloy, leading to changes in galvanic corrosion details and corrosion rate at the interface between aluminum matrix and second phase particles.

How to further reveal the corrosion process, product status, and impact assessment in the process of galvanic corrosion through reliable research methods have always been an important aspect of galvanic corrosion research. Aluminum alloys have high corrosion sensitivity due to their low corrosion potential in a wide range of applications. Although significant progress and breakthroughs have been made in the corrosion resistance of aluminum alloys [17–19], the corrosion mechanism of most aluminum alloys is still not completely understood. As early as 2001, Akid et al. [20] pointed out that the macroscopic methods used to measure galvanic corrosion (ZRA method and polarization curve method) obviously underestimated the sustainable current density of aluminum alloy/aluminum/steel coupling and designed the local scanning reference electrode technique (SRET) method to provide more detailed information of local corrosion current density through the corrosion current calibration program. With the development of scanning Kelvin probe force microscopy (SKPFM) and wire beam electrode (WBE), a powerful means of physical and chemical analysis has been provided for the study of the galvanic corrosion mechanism of aluminum alloys. At the same time, due to the complex interaction of many chemical processes, a complete understanding of local corrosion, such as the transport of corrosive substances, hydrolysis, precipitation, and accumulation of corrosion products, and the accompanying micro-galvanic pitting, is very difficult. Digital simulation can effectively simulate the corrosion process to study the influencing factors through theoretical derivation and numerical calculation in the corrosion process with high inhomogeneity and strong coupling characteristics, thereby providing an effective reference for mechanism exploration.

In this paper, firstly, the important role of micro-galvanic corrosion in the study of galvanic corrosion of aluminum alloy is introduced. Secondly, the influences of the material, geometric, and environmental medium properties of the galvanic pair, on the galvanic corrosion of aluminum alloy are introduced. Then the application of new experimental methods such as WBE, SKPFM, and first-principles calculation are discussed. Finally, the corrosion inhibition methods, such as anodic oxidation treatment, corrosion inhibitor treatment and coating protection, are introduced.

2 The Phenomenon of Description

The discovery of galvanic corrosion was first made by accident when Galvani was conducting frog dissection experiments. Galvani studied this thoroughly and published the experimental results in 1791 [21]. With the development of the times and the deepening of the research, the galvanic corrosion is generally studied as a condition of local corrosion according to the corrosion failure mode in modern times. Taking the liquid storage tank as an example, the tank holding the acidic liquid propellant (low corrosion potential aluminum alloy) is in close contact with the stainless steel pipe (high corrosion potential), coupled with the acidic electrolyte environment provided by the standing water. Under the existence of these three conditions, serious galvanic corrosion will occur between the two. The schematic diagram of the galvanic corrosion principle is shown in Fig. 1.
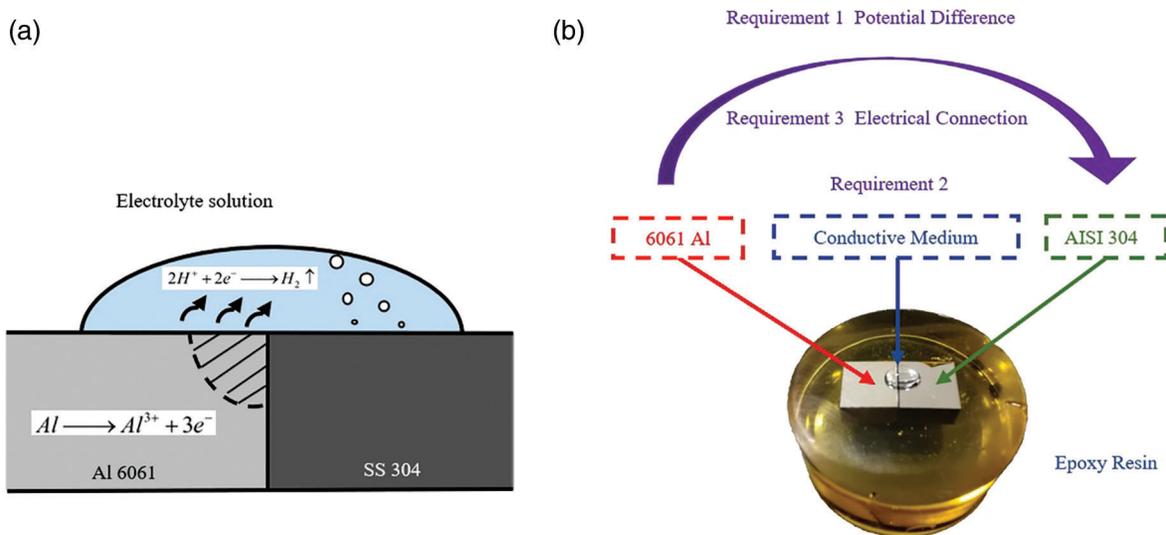

Figure 1: Brief schematic diagram of galvanic corrosion principle (a) Simulation diagram (b) Physical schematic diagram [21]

3 Corrosion Mechanism

3.1 Macroscopic Corrosion Mechanism

The macroscopic principle of galvanic corrosion can be explained by the corrosion galvanic principle and corrosion polarization diagram.

For example, in an acidic environment, the galvanic corrosion of aluminum alloy as anode and stainless steel as a cathode is taken as an example. The magnitude of its corrosion current is related to the electrode potential difference, polarizability, and circuit resistance of the two. If the corrosion current of the anodic aluminum alloy is written as i'_{Al}, then the galvanic corrosion effect γ is the ratio of i'_{Al} to i_{Al} (the corrosion current of the aluminum alloy when it is not coupled), as shown below:

$$\gamma = i'_{Al}/i_{Al} = (i_g + |i_{C,Al}|)/i_{Al} \approx i_g/i_{Al} \tag{1}$$

where i_g is the galvanic current density of aluminum alloy; $i_{C,Al}$ is the cathode reduction current density on aluminum alloy; The latter is usually small and negligible compared to the former. The larger the value of γ is, the more serious the galvanic corrosion is.

Based on the principle of galvanic corrosion, the principle of macroscopic galvanic corrosion can be further analyzed by a polarization diagram. It is assumed that the areas of the two metals are equal and that the cathodic process is only ion reduction. The respective conjugate electrode bodies on the two metal surfaces react as follows in Table 1:

Table 1: The electrode body reacts when aluminum alloy and stainless steel are coupled

	Oxidation reaction	Reduction reaction
Al	$Al \rightarrow Al^{3+} + 3e^-$	$2H^+ + 2e^- = H_2 \uparrow$
Fe	$Fe \rightarrow Fe^{2+} + 2e^-$	

Fig. 2 shows the polarization diagram of aluminum alloy with high potential and stainless steel with low potential before and after forming the galvanic pair.
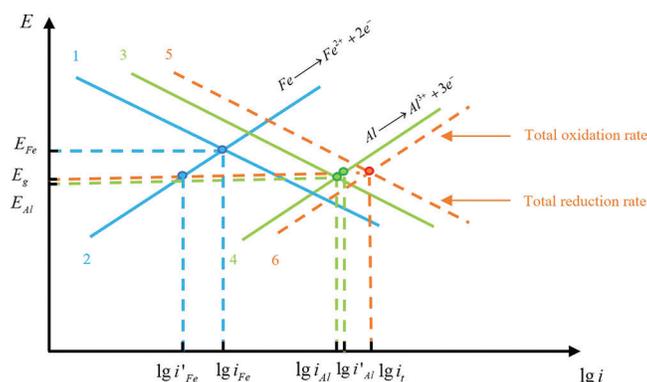

Figure 2: Corrosion polarization diagram

According to the polarization diagram, before the two metals are coupled, the intersection of the theoretical polar polarization curves of the metal Fe (line 1) and (line 2) determines its self-corrosion rate i_{Fe} and self-corrosion potential E_{Fe}. Similarly, the intersection of the theoretical anode Al (line 3) and anode (line 4) polar curves of a metal determines its self-corrosion rate i_{Al} and self-corrosion potential E_{Al}. When the two metals are coupled, according to the mixed potential theory, the intersection point of the total cathode polarization curve (5) and the total anode polarization curve (6) of the galvanic corrosion battery is the point where the total oxidation rate is equal to the total reduction rate. And it represents the total corrosion rate i_t and total mixed potential E_g (galvanic potential) of the coupling system, which is between E_{Fe} and E_{Al}. Due to the coupling effect, the corrosion current of metal Al increases from i_{Al} to i'_{Al}. That is, the anode polarization accelerates the corrosion. And the corrosion current of the metal Fe decreases from i_{Fe} to i'_{Fe}. That is, cathode polarization slows corrosion.

3.2 Micro Corrosion Mechanism

What needs to be distinguished is that the macroscopic galvanic corrosion mechanism focuses on the accelerated corrosion formed by the coupling of aluminum alloy and materials with different properties. The mechanism of microgalvanic corrosion emphasizes the galvanic corrosion between different microscopic particles on the surface of the same material. In the galvanic corrosion of aluminum alloy, it is reflected as the comprehensive effect of macroscopic dissimilar material driving force and microparticle driving force. However, regardless of macro and micro, it is the main direction in the field of galvanic corrosion of aluminum alloy to explore the specific role of microstructure and how to produce the effect. However, the technology of electrochemical testing of microzone can detect its electrochemical parameters and even in situ characterize its change process after the selected microzone is tested, and which better reflects the corrosion phenomenon and details of the microzone, has attracted increasing attention. The investigation of microcosmic corrosion mechanism is an important part of the establishment of a complete corrosion mechanism and has decisive significance for guiding the tracing of corrosion problems and the development of countermeasures for corrosion protection, is a hot field of aluminum alloy galvanic corrosion research.

From the aluminum alloy material itself, in the first aspect, modern aluminum alloys produce a large number of non-ideal products such as dendritic structures, intermediate phases and impurities during the production forging and hot working treatment. And these products will have a significant negative impact on the overall performance of aluminum alloys and limit their application scope to some extent [22]. It is difficult to predict the irregularity of impurities effectively, so it can be reasonably controlled by improving the processing technology and establishing the usage threshold in the production of aluminum alloy. In the second aspect, as an important part of aluminum alloy, the second phase particles of aluminum alloy can not only effectively affect the mechanical properties and strength properties of aluminum alloy, but also produce a non-negligible effect of microgalvanic corrosion in the process of coupling. The study on the microgalvanic corrosion of the second phase particles of aluminum alloy can effectively evaluate the effects of related particles, establish the corrosion process model, and predict the corrosion of materials.

According to the size, the particle composition of the second phase in the aluminum alloy is generally divided into three types, mainly precipitated phase, intermetallic compound particles (crystalline phase) and dispersion [23]. Take Al-Mg-Si alloy (corresponding to 6XXX series alloy [24]) as an example. Al-Mg-Si alloy not only has good formability, but also has high strength and corrosion resistance, and is widely used in equipment parts and parts processing fields [25]. According to relevant data [26–28], the precipitation sequence of Al-Mg-Si alloy treated effectively in industrial production is usually supersaturated solid solution (SSSS)→atomic cluster→GP region →β″ →β′, U1, U2, B′→β, Si. Studies have shown that the aging, hardening kinetics, and strength of Al-Mg-Si alloy can be effectively improved by increasing the density and Si content of Mg-Si clusters, GP region, and metastable Mg_2Si precipitated phase in the second phase particles [29,30]. The existence of these second phase particles not only changes the strength heterogeneity of Al-Mg-Si alloy microstructure, but also affects the heterogeneity of electrochemical properties, thus affecting the corrosion resistance of aluminum alloy [31]. As mentioned above, in the coarse second phase particles, the negative polar particles represented by Al_7Cu_2Fe and Al_2Cu have a positive volt potential relative to the aluminum matrix. In contrast, Mg_2Si, Al_2CuMg and other anodic particles have negative potentials. Driven by the corrosion potential difference, the microgalvanic corrosion caused by the coupling of these primary particles with the aluminum matrix is an important field to explore the mechanism of microgalvanic corrosion [32,33]. It has been pointed out in many publicly reported literature [34–37] that Mg_2Si particles in Al-Mg-Si alloy always undergo accelerated corrosion as local anodes in acidic pH solutions. Gharbi et al. [36] further pointed out when explaining the dissolution mechanism of Mg_2Si at different solution pH: When pH is 6,

Mg dissolves from Mg_2Si; When Si contacts with water, insoluble SiO_2 is formed, and a small part of it forms H_4SiO_4. Selective dissolution of Mg leads to enrichment of SiO_2 on the surface of Mg_2Si, and the schematic diagram of this mechanism is shown in Fig. 3.
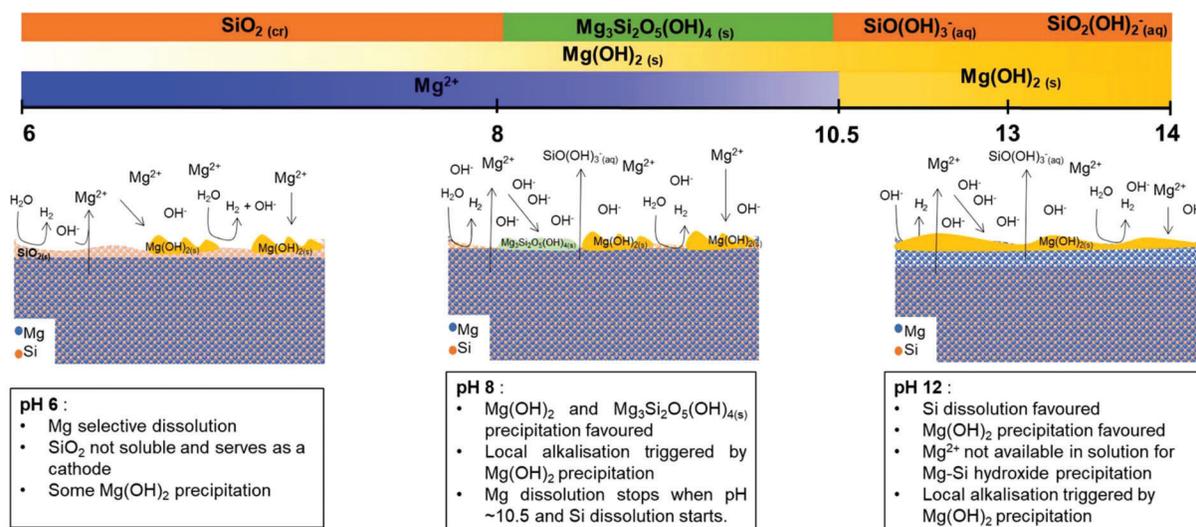

Figure 3: Schematic diagram of dissolution/precipitation mechanism of Mg_2Si [36]

Some studies have discussed the relationship between grain size and corrosion resistance after grain refinement, and the results show that reducing grain size can affect the corrosion resistance of materials, but the degree of influence is controversial [38]. Ralston et al. [39,40] believed that when the grain was refined, the material with oxide would slow down the corrosion rate. In aluminum alloy, the decomposition of the second phase particles will aggravate the corrosion degree.

In addition, the type and concentration of ions in corrosive media also play a crucial role in the study of the galvanic corrosion mechanism of aluminum alloy, among which the primary ions represented by Cl^- have the most important influence [41–43]. As shown in Fig. 4, Xue et al. [41] coupled LC4 alloy with different MAO film thickness with copper substrate for experiments and found that Cl^- in the solution would gradually penetrate into the membrane along the membrane defects, diffuse into the alloy matrix to form a dark corrosion zone, and gradually peel and peel off the film layer with the extension of test time, expanding and deepening the corrosion holes on the film surface. Sekularac et al. [43] pointed out that Cl^- would adsorb on the surface of aluminum alloy prior to O_2, leading to the unrepairable passivation film of aluminum alloy, thus increasing the pitting sensitivity of aluminum alloy.

4 Influencing Factor

There are many factors affecting the degree of corrosion. To facilitate the experimental study, the influencing factors of galvanic corrosion of aluminum alloy are mainly divided into three categories: the properties of galvanic material, the geometric properties of the galvanic pair, and the properties of the environmental medium. The schematic diagram is shown in Fig. 5.

4.1 Even Pair Material Properties

To retain the inherent characteristics of aluminum to significantly improve other properties, the industrial manufacturing process for aluminum alloy often resorts to pure aluminum organic doping copper, manganese, silicon, magnesium and other metals, and adopt a variety of processing technologies to forge

aluminum alloys to meet varying demands. According to the main alloy elements, China mainly uses the four-character system brand representation method to distinguish different types of aluminum alloy [44]. Mansfeld [45] conducted galvanic corrosion tests on five aluminum alloys (3.5% NaCl solution, $22 \pm 1°C$), and the results showed that the range was from -756 ± 39 mV *vs*. SCE to -814 ± 18 mV *vs*. SCE, and ranges from 0.24 to 0.95 mdd. Although the characteristics of different models of the same brand are slightly different, but there is a certain regularity. Therefore, the corrosion resistance of aluminum alloy is improved by adjusting the metal composition in the actual production process [46]. Hihara [47] showed that high resistivity reinforcement materials in aluminum matrix composites can significantly limit galvanic corrosion by increasing ohmic loss and formulated the selection of materials accordingly.
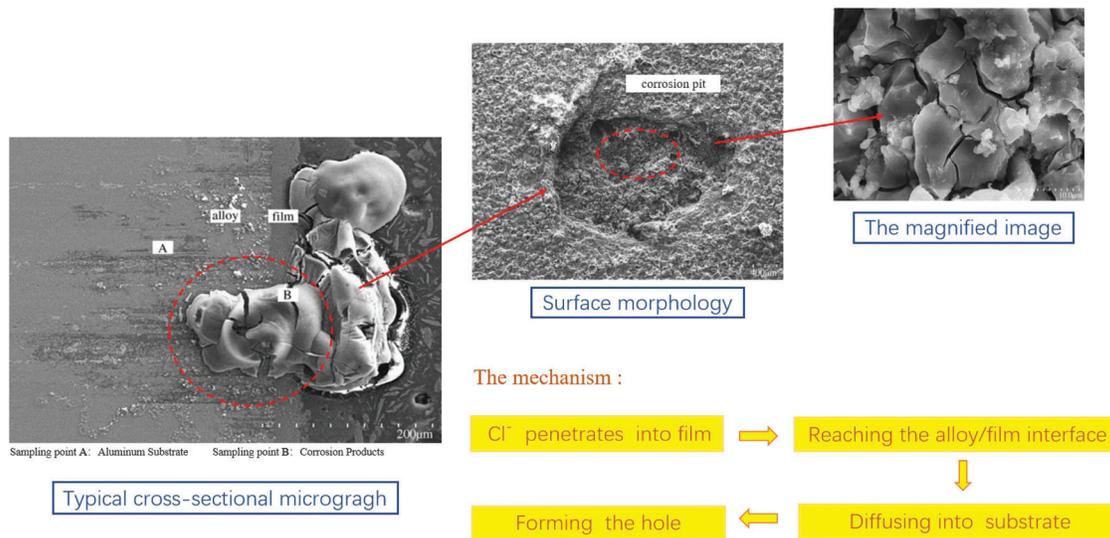

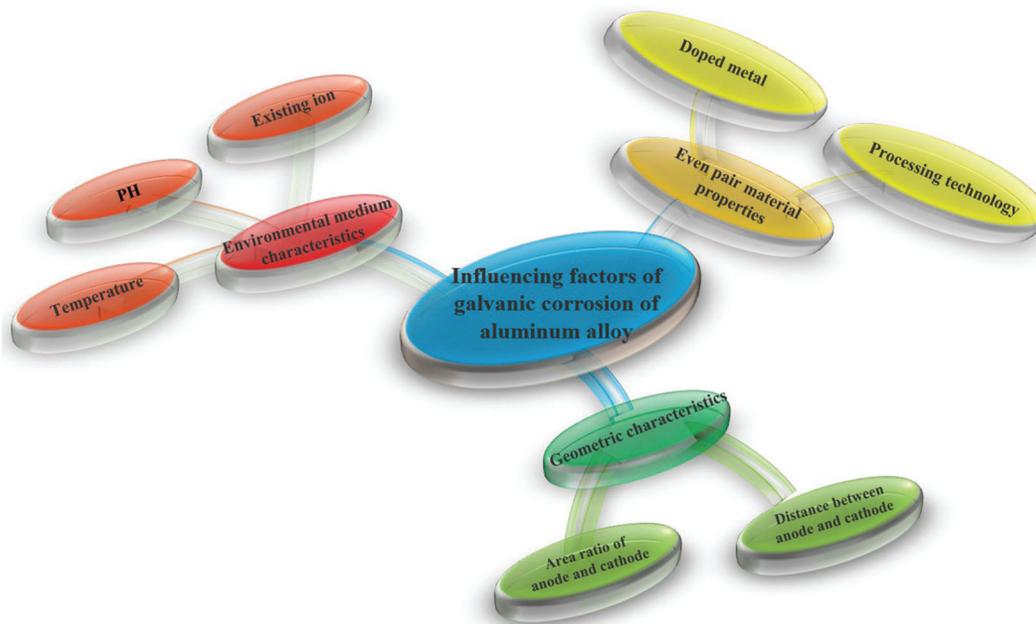**Figure 4:** Schematic diagram of Cl⁻ intrusion corrosion [41]

Figure 5: Schematic diagram of influencing factors of galvanic corrosion of aluminum alloy

4.2 Geometric Characteristics of Galvanic Pair

The coupling of aluminum alloy with stainless steel under acidic condition is taken as an example. When the anode reaction is controlled by active polarization and the cathode reaction by concentration polarization, the anode reaction in the cathode phase decreases to negligible, and the cathode reaction only occurs by default. The cathode reaction is not affected by the positive potential shift in the anode phase, that is, the cathode reaction velocity is still equal to the cathode diffusion current density.

The current relationship of the multiphase electrode is shown as follows [48]:

$$I_g = I_+(M_2) = S_2[i_a(M_2) - i_d] = |I_-(M_1)| = S_1 i_d \tag{2}$$

where I_g is the corrosion current, and $I_-(M_1)$ and $I_+(M_2)$ are the cathode current of stainless steel and anode current of aluminum alloy respectively, S_1 and S_2 are the effective area of stainless steel and aluminum alloy. $i_a(M_2)$ is the anodic corrosion current density of aluminum alloy, and i_d is the limit diffusion current density of depolarizing agent hydrogen ion.

After finishing, the anodic corrosion current density can be deduced as follows:

$$i_a(M_2) = i_d\left(1 + \frac{S_1}{S_2}\right) = i_{cor}(M_2)\left(1 + \frac{S_1}{S_2}\right) \tag{3}$$

where $i_{cor}(M_2)$ is the corrosion current density of aluminum alloy before coupling. The anodic corrosion current density is proportional to the area ratio of negative and positive electrodes. When the situation of "large cathode, small anode" occurs, the corrosion of anode is often more serious [49].

4.3 Environmental Medium Characteristics

The influence of the environmental medium on galvanic corrosion is most obviously reflected in the non-uniformity of anodic corrosion current. The closer it is to the junction of the galvanic pair, the smaller the resistance of the current path, and the larger the corrosion current density detected. Also, when the composition, temperature, pH, and other influencing factors of the environmental medium change, the change in corrosion behavior of the same galvanic pair will be affected [50] and a polarity reversal could occur. For example, aluminum metal and magnesium metal are coupled in a dilute neutral or acidic solution. At the beginning of corrosion, the magnesium metal electrode has a low potential and acts as a corrosion anode. When magnesium is dissolved, the solution turns alkaline, thus amphoteric aluminum metal turns into a corrosion anode [51]. The influence of primary ions in solution represented by Cl^- has been introduced previously, while the influence of associated ions represented by Al^{3+} also cannot be ignored. Some studies have shown that the dissolution of Al^{3+} from the electrode surface and the steric hindrance effect of material transport between the body solution and the anodic solution adjacent to the corrosion surface both affect the local pH and thus affect the local corrosion of aluminum alloy [52].

5 Test Standards and Research Methods

In practical research, because galvanic corrosion involves different materials and fields, its testing items and testing standards are also different. To save time and hasten the detection of the maximum degree of corrosion, a series of acceleration experiments are usually carried out within the error range allowed by the theory during the actual operation. These methods provide a strong basis for the investigation of the galvanic corrosion mechanism and protection detection of aluminum alloy.

5.1 Standard Test Method

Standard test methods commonly used in the study of galvanic corrosion of aluminum alloys mainly include HB 5374-1987, GB/T 19747-2005, ISO 7441:2015, ASTM G71-81(2019), and other general

standards. Some industry rules are also widely used because of their universality. For example, GB/T 15748-2013 of the shipping industry defines galvanic corrosion test methods for marine metals.

When the three preconditions are met/satisfied, the aluminum alloy will undergo galvanic corrosion with other materials. This creates an opportunity to maximize the use of actual environment as the test environment and has also attracted the attention of researchers. For example, ISO 2326:2020 can evaluate galvanic corrosion tests of aluminum alloys exposed in deep-sea environments; ISO 21746:2019 evaluates galvanic corrosion behavior of aluminum alloys and carbon fiber reinforced plastics (CFRPs) in a salt spray environment. With the development of technology, the corresponding test standards for new detection technology are also followed up. Taking the multi-electrode array technique for local area measurement as an example, ISO 23449:2020 specifies the inhibitors used after screening, the galvanic current and potential distribution of different metal pairs for evaluating metals of different compositions and properties in different environments.

5.2 The Research Methods

5.2.1 Traditional Electrochemical Technology

Electrochemical measurement can give real-time information on corrosion and continuously track the corrosion of the electrode surface [53]. In the traditional electrochemical measurement of galvanic corrosion of aluminum alloys, three electrodes are often used to test the target material. Traditional electrochemical measurement methods include the open circuit potential (OCP) method, the potentiodynamic polarization (PDP) method, and the AC impedance (EIS) method.

The open circuit potential (OCP) method mainly measures the electrode potential of materials with no current. In this type of experiment, the counter pair electrode is usually regarded as the working electrode and the counter electrode respectively and the corrosion potential difference between aluminum alloy and dissimilar metal is measured to judge the tendency of the couple corrosion between the pair [54]. In the process of polarization, the surface state of the pair is difficult to stabilize, so the potentiodynamic polarization (PDP) method adopting the potential ladder method or potential scanning method is often used to measure the relationship between self-corrosion potential and corrosion current density. The steady-state polarization curve of aluminum alloy is commonly measured by the potentiostatic method, and the ICORR is obtained by Tafel extrapolation in the strong polarization region [55]. The equilibrium potential and corrosion current of the polarization curve can be obtained by the B-V equation and Tafel formula. At the same time, the corrosion rate of aluminum alloy can be calculated according to the polarization curve. Compared with the previous two methods, the unstable method is gradually becoming popular because it effectively considers several parameters, including time dependence. The main trend in testing and analysis in the frequency domain is the AC impedance (EIS) method, which is often combined with the equivalent circuit to obtain the dynamic information and the information on the electrode interface structure. Steven et al. [56] studied the galvanic corrosion current analysis between aluminum alloy and stainless steel exposed to balanced electrolytic droplets and obtained the baseline corrosion kinetic information of the two alloys through EIS measurement. The Kramers-Kronig residuals of UNS S13800 and UNS A97075 samples show that the response of aluminum alloy to potential perturbation is linear.

Due to the properties of aluminum alloy and the influence of temperature, pH, electrolyte solution impedance, and other conditions, material passivation and galvanic polarity reversal often occur in practical applications. This is not accurately reflected by the average electrochemical parameters obtained from traditional electrochemical measurements. Therefore, the following will introduce micro-electrochemical measurement, digital simulation, and other new research techniques.

5.2.2 Wire Beam Electrodes (WBE) Technology

The multi-electrode array technology mentioned above, often called the Wire Beam electrode (WBE) technology, was based on the principle of forming a complete electrode by combining a certain number of individual electrodes insulated from each other in a specific arrangement [57]. Because it uses calculus to transform macroscopic electrochemical parameters into the organic coupling of electrochemical parameters in small areas, it can reflect the differences of electrochemical properties in different areas on the surface of aluminum alloy coupling and can effectively extract the corrosion characteristics and preferred corrosion areas of aluminum alloy galvanic corrosion through analysis. It is of great significance to explore the mechanism and process of complex galvanic corrosion of aluminum alloy [58]. Shi et al. [49] used array electrode technology to explore the galvanic corrosion behavior of trimetals and found that the dielectric environment in 3.5 wt.% NaCl solution had a high conductivity, and the spatial arrangement of electrodes had little impact on the galvanic corrosion of trimetals. Therefore, a new splice array electrode was needed to be designed for measurement. Meanwhile, as the size of a single electrode is in the order of millimeters, other measurement methods such as optical microscopy and Raman spectroscopy can be coupled to improve the measurement accuracy of WBE [59,60].

5.2.3 Scanning Kelvin Probe Force Microscopy (SKPFM) Technology

Scanning Kelvin Probe Force Microscopy (SKPFM) technology, as a derivative of atomic Force Microscopy (AFM), has the advantages of nanometer resolution and high energy sensitivity compared with WBE technology. It is widely used to characterize regional electrochemical inhomogeneity and to evaluate the electrochemical behavior of various second phase particles. Schmutz et al. [61] pointed out that the potential value of pure metal measured by SKPFM had a linear relationship with the open circuit potential in solution, and the intermetallic compound particles showed a clear volt potential contrast with the matrix. It should be noted that the potential function or work function mapping obtained by SKPFM is often affected by important topographic artifacts, and the measured values are greatly influenced by the cantilever position. As shown in Fig. 6, on the same rough surface of the specimen, when the cantilever beam detection position A and B are slightly different, the data measured by the probe tip is not uniform, and inversion may even be observed [62,63]. With the development of digital simulation technology, SKPFM measurement results are often verified with simulation model results such as first-principles calculation to obtain a more accurate and reliable reaction path analysis [64].
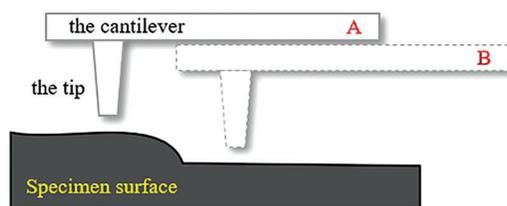

Figure 6: Schematic diagram of influence of cantilever beam position on detection (where A and B are different test locations)

5.2.4 First Principles Calculations

The galvanic corrosion of aluminum alloy is often crosslinked with stress corrosion and other corrosion conditions [65,66], and the influencing factors include environment, material, and other aspects. It is very difficult to fully understand the corrosion process through technical detection. The first principle obtains the physical and chemical properties of microscopic particles by solving the Schrodinger equation [67], which has been widely used in reaction construction, mechanism research, and corrosion prediction of aluminum alloy galvanic corrosion. Density Functional Theory (DFT) in first-principles calculation is

commonly used to calculate lattice constants and crystal plane parameters of microscopic particles in the corrosion process [68]. Fall et al. [69] showed here that a technique based on macroscopic averages can be used to reduce such effects and determine more precisely the work functions of metals from ab initio thin-film calculations. And the method is applied to Al(100) slabs containing 1–14 atomic layers. It is worth noting that most of the surface simulated by the current DFT calculation is not adsorbed or oxidized, while in practical application, real aluminum alloy often has oxide film or coating, which leads to some deviation in the coincidence degree between the theoretical calculation results and the actual measurement results. In order to improve the practical applicability and prediction accuracy of the model, other methods can be tried to combine DFT for corrosion prediction [67].

6 Research in the Field of Corrosion Inhibition

As one of the most valuable derivative fields, aluminum alloy corrosion inhibition has a certain foundation after many years of research. To effectively alleviate the galvanic corrosion of aluminum alloy, the commonly used corrosion inhibition methods at present mainly include optimized material selection and structural design, anodic oxidation treatment, corrosion inhibitor treatment, coating protection and so on.

Under natural conditions, the surface of aluminum and its alloy will spontaneously form a natural alumina protective film about 2~3 nm thick [70]. However, due to the instability and relative vulnerability of natural oxide film, anodic oxidation technology is often used in practice to obtain the ideal structure and thickness of oxide film structure. According to the different preparation methods, the anodic alumina (AAO) membrane can be divided into two types: barrier type and multi-pass type [71]. It should be noted that the temperature and pH of the electrolyte should be kept within a small range during the anodic oxidation process; otherwise, the pore shape, geometric size and stack thickness on the surface will be distributed unevenly [72]. On the original basis, micro-arc oxidation (MAO) technology can generate ceramic oxide film on aluminum alloy through arc light discharge, which has better wear resistance and corrosion resistance [73]. Hua et al. [74] studied the corrosion behavior of 7050 aluminum alloy after micro-arc oxidation under constant load and different pH environments and found that its oxidation film showed different corrosion laws under different conditions.

The corrosion inhibitor can form adsorption film or product film through reaction to prevent further contact between aluminum alloy and corrosive medium, which is a simple, effective, and feasible means of protection. Commonly used corrosion inhibitors for aluminum alloys mainly include organic, inorganic, and rare earth corrosion inhibitors [75]. Organic corrosion inhibitors represented by alkyl amines, thioureas and aldehydes can provide multiple attachment sites to form insoluble blocking reactions on metal surfaces. Chromate, vanadate, permanganate and so on are representative inorganic corrosion inhibitors, and their specific mechanisms differ according to different ion types. Taking chromate as an example, CrO_4^{2-} can be reduced to produce $Cr(OH)_3$ to repair aluminum alloy passivation film [76]. Commonly used rare earth corrosion inhibitors are mainly lanthanum and cerium salts, and their mechanism is mainly through the formation of oxides and hydroxides to isolate the corrosive surface. However, improvement of the inhibition efficiency is an important problem with rare earth corrosion inhibitors. Tan et al. [77] pointed out that when the concentration is 1000 ppm, $LaCl_3$ can significantly inhibit the local corrosion of AA2024-T3, resulting in a decrease of its local current, as shown in Fig. 7. But at the same time, the inhibition behavior cannot suppress the overall corrosion. Moreover, when the concentration drops to 500 ppm, its efficiency decreases sharply, and the inhibitory effect of this process cannot be improved by adding $LaCl_3$.

Chromate, a commonly used corrosion inhibitor for aluminum alloy, is carcinogenic [78]. So, finding a new non-toxic, harmless, green, and healthy corrosion inhibition method has become a hot research field. Coating technology doped with specific inhibitors combines the advantages of both and has broad application prospects. Tsai et al. [78], and Shruthi et al. [79], respectively, conducted experiments on the anticorrosion coating technology of aviation aluminum alloy. Marshall et al. [80], through finite element

simulation, calculated relevant parameters after the coupling of coated aluminum alloy and stainless steel. It should be noted that most studies have pointed out the average response of coatings, but the influence of pinhole paint heterogeneity and damage of tiny scratches on the difference of coating reactivity needs further research [81]. New materials such as nanomaterials and graphene materials also provide new research ideas for the preparation of coatings. Zhu et al. [82] summarized the research progress of graphene anticorrosive coating and pointed out its corrosion promotion behavior and corresponding countermeasures.
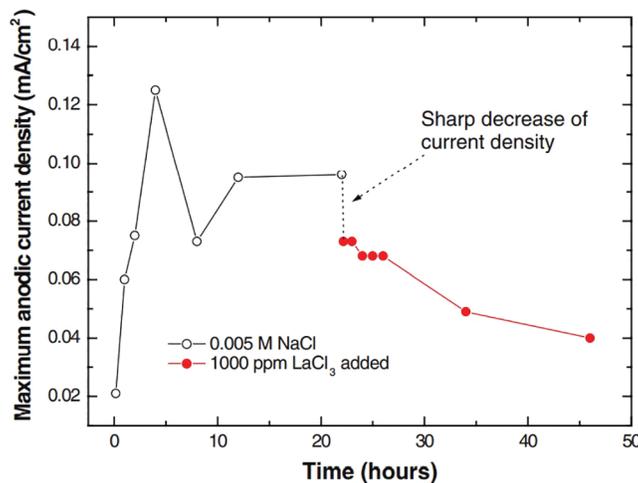

Figure 7: Diagram of maximum anode current density changing after adding 1000 ppm $LaCl_3$ [67]

7 Conclusion

With the development of construction infrastructure, fuel storage, deep-sea exploration and other activities, galvanic corrosion of aluminum alloy has attracted extensive attention as a common problem. In this review, we find that the current research on galvanic corrosion of aluminum alloy has the following characteristics:

(1) The investigation on the principle of galvanic corrosion of aluminum alloy has been deepened from macro to micro. The galvanic corrosion mechanism of aluminum alloy, which focuses on whether and how particles in the micro region participate in the reaction, has become the mainstream. At the same time, due to the difference of materials and working environment, the study of galvanic corrosion of aluminum alloy is mainly carried out on the properties of pair materials, the geometric properties of galvanic pair and the characteristics of environmental media.

(2) At present, a relatively perfect standard system for galvanic corrosion testing of aluminum alloy has been established, and relevant requirements have been made for the standardization of some special environments and new research methods. The new research methods represented by WBE technology, SKPFM technology, and first-principles calculation provide a good method to obtain information on micro-area corrosion parameters, establish a corrosion process model, and predict the corrosion degree of aluminum alloy.

(3) Aluminum alloy corrosion inhibition technology represented by anodic oxidation treatment, corrosion inhibitor treatment, and coating protection has undergone considerable development and progress, making an important contribution to saving resources and reducing costs. The combination of new technologies such as arc light discharge, and new materials such as

nanomaterials, to develop new non-toxic, harmless, efficient, and energy-saving corrosion inhibition has become the main goal of aluminum alloy corrosion inhibition research.

Conflicts of Interest: The authors declare that they have no conflicts of interest to report regarding the present study.

References

1. David, E. J. T., James, D. R. T. (2007). *Corrosion science and technology.* Second edition. UK: Taylor & Francis Group.

2. Jonathan, W. (2015). *Rust: The longest war.* USA: Simon & Schuster.

3. Richards, J. W. (1895). The resistance to corrosion of some light aluminium alloys. *Journal of the Franklin Institute, 139(1),* 69–72. https://doi.org/10.1016/0016-0032(95)90097-7

4. Torbati, S. H., Torbati, S. S. A., Chawla, N., Poursaee, A. (2020). A comparative study of corrosion behavior of an additively manufactured Al-6061 RAM2 with extruded Al-6061 T6. *Corrosion Science, 174.* https://doi.org/10.1016/j.corsci.2020.108838

5. Zhu, X. R., Huang, G. Q. (1994). Research of contact corrosion of metallic materials in sea water. *Marine Sciences, 6,* 55–59.

6. Collicott, S. H., Yendler, B. (2022). Asymmetric propellant positioning in symmetric tanks and propellant management devices. *Journal of Spacecraft and Rockets, 59(2),* 482–488. https://doi.org/10.2514/1.A35095

7. Ruiz, G. A., Jimenez, G. E., Cano, E., Mayen, M. R., Genesca, J. et al. (2019). The corrosion products in a carbon steel/aluminum alloy galvanic couple under thin electrolyte films: An efficient model. *Electrochemistry Communications, 104,* 106485. https://doi.org/10.1016/j.elecom.2019.106485

8. Sidane, D., Bousquet, E., Devos, O., Puiggali, M., Touzet, M. et al. (2014). Local electrochemical study of friction stir welded aluminium alloy assembly. *Journal of Electroanalytical Chemistry, 737,* 206–211. https://doi.org/10.1016/j.jelechem.2014.06.025

9. João, C. B., Sara, M. M., Luís, F. P. (2015). Corrosion study of the friction stir lap joint of AA7050-T76511 on AA2024-T3 using the scanning vibrating electrode technique. *Corrosion Science, 94,* 359–367. https://doi.org/10.1016/j.corsci.2015.02.029

10. Uyime, D., Rejane, M. P., João, V., Milagre, M. X., Abreu, C. P. (2019). Macro and microgalvanic interactions in friction stir weldment of AA2198-T851 alloy. *Journal of Materials Research and Technology, 8(6),* 6209–6222. https://doi.org/10.1016/j.jnart.2019.10.015

11. Mariana, X. M., Uyime, D., Naga, V., Rejane, M. P. S., Bárbara, V. G. D. V. et al. (2020). Galvanic and asymmetry effects on the local electrochemical behavior of the 2098-T351 alloy welded by friction stir welding. *Journal of Materials Science & Technology, 45(10),* 162–175. https://doi.org/10.1016/j.jmst.2019.11.016

12. Silva, D., Rejane, M. P., Araujo, D. S., Xavier, M. M. (2021). On the local corrosion behavior of coupled welded zones of the 2098-T351 Al-Cu-Li alloy produced by Friction Stir Welding (FSW): An amperometric and potentiometric microelectrochemical investigation. *Electrochimica Acta, 373,* 137910. https://doi.org/10.1016/j.electacta.2021.137910

13. Silva, D., Izquierdo, J., Milagre, M. X., Antunes, R. A., Souto, R. M. et al. (2022). Development of an Al^{3+} ion-selective microelectrode for the potentiometric microelectrochemical monitoring of corrosion sites on 2098−T351 aluminum alloy surfaces. *Electrochimica Acta, 415,* 140260. https://doi.org/10.1016/j.electacta.2022.140260

14. El-Garhy, G., Mahallawy, E. N., Shoukry, M. K. (2021). Effect of grain refining by cyclic extrusion compression (CEC) of Al-6061 and Al-6061/SiC on wear behavior. *Journal of Materials Research and Technology, 12,* 1886–1897. https://doi.org/10.1016/j.jmrt.2021.03.114

15. Campestrini, P., Westing, E., Rooijen, H. (2013). Relation between microstructural aspects of AA2024 and its corrosion behaviour investigated using AFM scanning potential technique. *Corrosion Science, 42(11),* 1853–1861. https://doi.org/10.1016/S0010-938X(00)00002-0

16. Andreatta, F., Terryn, H., Wit, J. (2003). Effect of solution heat treatment on galvanic coupling between intermetallics and matrix in AA7075-T6. *Corrosion Science, 45(8),* 1733–1746. https://doi.org/10.1016/S0010-938X(03)00004-0

17. Roland, T. L. (2020). Corrosion resistance of 3105 and 6110 aluminium alloy in neutral chloride- and sulphate-contaminated artificial seawater. *Journal of Bio- and Tribo-Corrosion, 6(4),* 705–736. https://doi.org/10.1007/s40735-020-00406-2

18. Verdalet, G. X., Saillard, R., Fori, B., Duluard, S., Blanc, C. (2020). Comparative analysis of the anticorrosive properties of trivalent chromium conversion coatings formed on 2024-T3 and 2024-T351 aluminum alloys. *Corrosion Science, 167,* 108508. https://doi.org/10.1016/j.corsci.2020.108508

19. Sravanthi, S. S., Acharyya, S. G., Joardar, J., Chaitanya, V. N. S. K. (2020). A study on corrosion resistance and mechanical performance of 6061 aluminium alloy: Galvanized mild steel electron beam welds at varying welding parameters. *Transactions of the Indian Institute of Metals, 73(4),* 881–895. https://doi.org/10.1007/s12666-020-01893-0

20. Akid, R., Mills, D. J. (2001). A comparison between conventional macroscopic and novel microscopic scanning electrochemical methods to evaluate galvanic corrosion. *Corrosion Science, 43(7),* 1203–1216. https://doi.org/10.1016/S0010-938X(00)00091-3

21. Galvani, L. (1791). De viribus electricitatis in motu musculari commentarius. *Bologna Accademia Delle Scienze, 7,* 363–418.

22. Pan, L., Zhang, Q. H., Hu, J. M., Cao, F. H. (2021). Interesting phenomena for Al-Zn-Mg aluminum alloy after two years of storage: A comparative study on microstructure, mechanical properties, and corrosion behavior of aluminum alloy with different aging treatments. *Construction and Building Materials, 276,* 122210. https://doi.org/10.1016/j.conbuildmat.2020.122210

23. Birbilis, N., Buchheit, R. G. (2005). Electrochemical characteristics of intermetallic phases in aluminum alloys an experimental survey and discussion. *Journal of the Electrochemical Society, 152(4),* B140–B151. https://doi.org/10.1149/1.1869984

24. Li, X. C. (2019). *Microstructure and metallographic atlas of aluminum alloy.* China: Metallurgical Industry Press.

25. Ardell, A. J. (1985). Precipitation hardening. *Metallurgical Transactions A, 16,* 2131–2165. https://doi.org/10.1007/BF02670416

26. Edwards, G. A., Stiller, K., Dunlop, G. L. (1998). The precipitation sequence in Al-Mg-Si alloys. *Acta Materialia, 46(11),* 3893–3904. https://doi.org/10.1016/S1359-6454(98)00059-7

27. Wenner, S., Jones, L., Marioara, C. D., Holmestad, R. (2017). Atomic-resolution chemical mapping of ordered precipitates in Al alloys using energy-dispersive X-Ray spectroscopy. *Micron, 96,* 103–111. https://doi.org/10.1016/j.micron.2017.02.007

28. Moharami, A., Razaghian, A., Babaei, B., Ojo, O., Slapakova, M. (2020). Role of Mg_2Si particles on mechanical, wear, and corrosion behaviors of friction stir welding of AA6061-T6 and Al-Mg_2Si composite. *Journal of Composite Materials, 54(26),* 4035–4057. https://doi.org/10.1177/0021998320925528

29. Maruyama, N., Uemori, R., Hashimoto, N., Saga, M., Kikuchi, M. (1997). Effect of silicon addition on the composition and structure of fine-scale precipitates in Al-Mg-Si alloys. *Scripta Materialia, 36(1),* 89–93. https://doi.org/10.1016/S1359-6462(96)00358-2

30. Marioara, C. D., Andersen, S. J., Zandbergen, H. W., Holmestad, R. (2005). The influence of alloy composition on precipitates of the Al-Mg-Si system. *Metallurgical & Materials Transactions A, 36(3),* 691–702. https://doi.org/10.1007/s11661-005-1001-7

31. Kairy, S. K., Birbilis, N. (2020). Clarifying the role of Mg_2Si and Si in localised corrosion of Al-alloys by Quasi in-situ transmission electron microscopy. *Corrosion, 76(5),* 464–475. https://doi.org/10.5006/3457

32. Liu, Y., Zhang, X. M., Zhang, H. (2013). Role of secondary phase particles of 2519A aluminium alloy in localised corrosion. *Materials Research Innovations, 17(Supplement1),* 83–88. https://doi.org/10.1179/1432891713Z.000000000187

33. Gharbi, O., Kairy, S. K., Lima, P. R., Jiang, D., Nicklaus, J. et al. (2019). Microstructure and corrosion evolution of additively manufactured aluminium alloy AA7075 as a function of ageing. *npj Mater Degradation, 3(1),* 151–186. https://doi.org/10.1038/s41529-019-0101-6

34. Eckermann, F., Suter, T., Uggowitzer, P. J., Afseth, A., Schmutz, P. (2008). The influence of MgSi particle reactivity and dissolution processes on corrosion in Al-Mg-Si alloys. *Electrochimica Acta, 54(2),* 844–855. https://doi.org/10.1016/j.electacta.2008.05.078

35. Gupta, R. K., Sukiman, N. L., Fleming, K. M. (2012). Electrochemical behavior and localized corrosion associated with Mg_2Si particles in Al and Mg alloys. *ECS Electrochemistry Letters, 1(1),* C1–C3. https://doi.org/10.1149/2.002201eel

36. Gharbi, O., Birbilis, N. (2018). Clarifying the dissolution mechanisms and electrochemistry of Mg_2Si as a function of solution pH. *Journal of the Electrochemical Society, 165(9),* C497–C501. https://doi.org/10.1149/2.1061809jes

37. Guillaumin, V., Mankowski, G. (2000). Localized corrosion of 6056 T6 aluminium alloy in chloride media. *Corrosion Science, 42(1),* 105–125. https://doi.org/10.1016/S0010-938X(99)00053-0

38. Aziz, K. A., Ahmed, E. M., Alghtani, A. H., Felemban, B. F., Ali, H. T. et al. (2021). Development of Al-Mg-Si alloy performance by addition of grain refiner Al-5Ti-1B alloy. *Science Progress, 104(2),* 1–15. https://doi.org/10.1177/00368504211029469

39. Ralston, K. D., Birbilis, N., Davies, C. H. J. (2010). Revealing the relationship between grain size and corrosion rate of metals. *Scripta Metallurgica, 63(12),* 1201–1204. https://doi.org/10.1016/j.scriptamat.2010.08.035

40. Ralston, K. D., Birbilis, N. (2010). Effect of grain size on corrosion: A review. *Corrosion, 66(7),* 075005-1–075005-13. https://doi.org/10.5006/1.3462912

41. Xue, W. B., Wang, C., Tian, H., Lai, Y. C. (2006). Corrosion behaviors and galvanic studies of microarc oxidation films on Al-Zn-Mg-Cu alloy. *Surface and Coatings Technology, 201(21),* 8695–8701. https://doi.org/10.1016/j.surfcoat.2006.10.029

42. Sakairi, M., Otani, K., Sasaki, R. (2014). Electrochemical noise evaluation of metal cation effects on galvanic corrosion of aluminum alloys in low concentration of chloride ion containing solutions. *Procedia Engineering, 86,* 589–596. https://doi.org/10.1016/j.proeng.2014.11.084

43. Sekularac, G., Milosev, I. (2018). Corrosion of aluminium alloy AlSi7Mg0.3 in artificial sea water with added sodium sulphide. *Corrosion Science, 144,* 54–73. https://doi.org/10.1016/j.corsci.2018.08.038

44. Lin, G., Lin, H. G., Zhao, Y. T. (2006). *Aluminum alloy application manual.* China: China Machine Press.

45. Mansfeld, F. (1974). Galvanic corrosion of Al alloys. *Materials & Corrosion, 25(8),* 578–586. https://doi.org/10.1002/maco.19740250804

46. Pei, Z. H. (2012). Comparative, research of galvanic corrosion of 2024 and 2124 aluminum ally. *Journal of Chinese Society for Corrosion and Protection, 32(2),* 133–136.

47. Hihara, L. H. (1997). Corrosion of aluminium-matrix composites. *Corrosion Reviews, 15,* 3–4. https://doi.org/10.1515/CORRREV.1997.15.3-4.361

48. Gong, M., Yu, Z. X., Chen, L. (2020). *Metal corrosion theory and corrosion control.* China: Chemical Industry Press.

49. Shi, L. J., Song, Y. W., Zhao, P. P., Wang, H. T., Dong, K. H. et al. (2020). Variations of galvanic currents and corrosion forms of 2024/Q235/304 tri-metallic couple with multivariable cathode/anode area ratios: Experiments and modeling. *Electrochimica Acta, 359,* 136947. https://doi.org/10.1016/j.electacta.2020.136947

50. Sarah, L., Mathilde, L., Kimberly, C., Kapusta, B., Delpech, S. et al. (2020). Effects of temperature and pH on uniform and pitting corrosion of aluminium alloy 6061-T6 and characterisation of the hydroxide layers. *Journal of Alloys and Compounds, 833,* 155146. https://doi.org/10.1016/j.jallcom.2020.155146

51. Kong, X. D., Hu, H. E., Su, X. H. (2016). *Introduction to metal corrosion and protection.* China: Science Press.

52. Yin, L. T., Li, W. C., Wang, Y. C., Jin, Y., Pan, J. S. et al. (2019). Numerical simulation of micro-galvanic corrosion of Al alloys: Effect of density of Al(OH)$_3$ precipitate. *Electrochimica Acta, 324,* 134847. https://doi.org/10.1016/j.electacta.2019.134847

53. Thompson, A. H. (1997). Electrochemical potential spectroscopy: A new electrochemical measurement. *Journal of the Electrochemical Society, 126(4),* 608–616. https://doi.org/10.1149/1.2129095

54. Anaman, S. Y., Cho, H. H., Das, H., Baik, S., Hong, S. T. et al. (2019). Galvanic corrosion assessment of friction stir butt welded joint of aluminum and steel alloys. *International Journal of Precision Engineering and Manufacturing-Green Technology, 7(4),* 2288–6206. https://doi.org/10.1007/s40684-019-00183-5

55. McCafferty, E. (2005). Validation of corrosion rates measured by the Tafel extrapolation method. *Corrosion Science, 47(12),* 3202–3215. https://doi.org/10.1016/j.corsci.2005.05.046

56. Steven, A. P., Anderson, R. M., Carlos, M. H. (2021). Analysis of galvanic corrosion current between an aluminum alloy and stainless-steel exposed to an equilibrated droplet electrolyte. *Journal of the Electrochemical Society, 168(4),* 041507. https://doi.org/10.1149/1945-7111/abf5a7

57. Eren, H., Lowe, A. M., Tan, Y. J., Bailey, S. I., Kinsella, B. (1998). An auto-switch for multisampling of a wire beam electrode corrosion monitoring system. *IEEE Transactions on Instrumentation and Measurement, 47(5),* 1096–1101. https://doi.org/10.1109/19.746563

58. Nakatsugawa, I., Chino, Y. (2021). Effect of area ratio on the galvanic corrosion of AZX611 magnesium alloy/A6N01 aluminum alloy joint. *Materials Transactions, 62(12),* 1764–1770. https://doi.org/10.2320/matertrans.MT-L2021011

59. Battocchi, D., He, J., Bierwagen, G. P., Tallman, D. E. (2005). Emulation and study of the corrosion behavior of Al alloy 2024-T3 using a wire beam electrode (WBE) in conjunction with scanning vibrating electrode technique (SVET). *Corrosion Science, 47(5),* 1165–1176. https://doi.org/10.1016/j.corsci.2004.06.021

60. Qi, J. T., Wang, X. X., Ye, Z. H., Sun, W. T., Mu, H. T. (2021). Exploration on application of fiber beam electrode coupled optical microscope in professional experiment teaching. *Experimental Technology and Management, 38(5),* 83–88. https://doi.org/10.16791/j.cnki.sjg.2021.05.017

61. Schmutz, P., Frankel, G. S. (1998). Characterization of AA2024-T3 by scanning Kelvin probe force microscopy. *Journal of the Electrochemical Society, 145(7),* 2285–2295. https://doi.org/10.1149/1.1838633

62. Rohwerder, M., Turcu, F. (2008). High-resolution Kelvin probe microscopy in corrosion science: Scanning Kelvin probe force microscopy (SKPFM) versus classical scanning Kelvin probe (SKP). *Electrochimica Acta, 53(2),* 290–299. https://doi.org/10.1016/j.electacta.2007.03.016

63. Mcmurray, H. N., Williams, G. (2002). Probe diameter and probe-specimen distance dependence in the lateral resolution of a scanning Kelvin probe. *Journal of Applied Physics, 91(3),* 1673–1679. https://doi.org/10.1063/1.1430546

64. Qin, Y. F., Wang, S. Q. (2015). Ab-initio study of the role of Mg$_2$Si and Al$_2$CuMg phases in electrochemical corrosion of Al alloys. *Journal of the Electrochemical Society, 162(9),* C503–C508. https://doi.org/10.1149/2.0311509jes

65. Ni, L., Chao, F. D., Chen, M., Yao, J. Z. (2019). In situ electrochemical atomic force microscopy and auger electro spectroscopy study on the passive film structure of 2024-T3 aluminum alloy combined with a density functional theory calculation. *Advanced Engineering Materials, 21,* 1900386. https://doi.org/10.1002/adem.201900386

66. Cui, T. F., Liu, D. X., Shi, P. A., Yi, Y. H., Zhou, H. L. et al. (2018). Effect of stress and galvanic factors on the corrosion behavior of aluminum alloy. *Journal of Wuhan University of Technology-Mater. Sci. Ed., 33(3),* 688–696. https://doi.org/10.1007/s11595-018-1879-8

67. Ni, L., Chao, F. D., Chen, M., Li, X., Kong, D. C. et al. (2020). Insight into the localized strain effect on micro-galvanic corrosion behavior in AA7075-T6 aluminum alloy. *Corrosion Science, 180,* 109174. https://doi.org/10.1016/j.corsci.2020.109174

68. Hohenberg, P., Kohn, W. (1964). Inhomogeneous electron gas. *Physical Review, 136(3B),* B864. https://doi.org/10.1103/PhysRev.136.B864

69. Fall, C. J., Binggeli, N., Baldereschi, A. (1999). Deriving accurate work functions from thin-slab calculations. *Journal of Physics: Condensed Matter, 11,* 2689–2696. https://doi.org/10.1088/0953-8984/11/13/006

70. Cabrera, N., Mott, N. F. (1949). Theory of the oxidation of metals. *Reports on Progress Physics, 12(1),* 163–184. https://doi.org/10.1088/0034-4885/12/1/308

71. Zhang, F., Nilsson, J. O., Pan, J. S. (2016). In situ and operando AFM and EIS studies of anodization of Al 6060: Influence of intermetallic particles. *Journal of the Electrochemical Society, 163(9),* C609–C618. https://doi.org/10.1149/2.0061610jes

72. Hu, L. F., Chen, D. M., Shi, F. R., Chen, S. P. (2016). Effect of AlSiFe on the anodizing process of 6063 aluminum. *Surface and Interface Analysis, 48(12),* 1299–1304. https://doi.org/10.1002/sia.6036

73. Wang, H. J., Chen, G., Wu, Y., Yang, X. Y. (2022). Preparation and corrosion behavior of self-repairing micro arc oxidation film on 6061 aluminum alloy. *Ordnance Material Science and Engineering, 45(1)*. https://doi.org/10.14024/j.cnki.1004-244x.20210824.003

74. Hua, T. S., Song, R. G., Zong, Y., Cai, S. W. (2020). Corrosion behavior of 7050 aluminum alloy after micro-arc oxidation under constant load in NaCl solution with different pH values. *Surface Technology, 49(5),* 269–278. https://doi.org/10.16490/j.cnki.issn.1001-3660.2020.05.032

75. Semiletov, A. M., Makarychev, Y. B., Chirkunov, A. A., Kazansky, L. P., Kuznetsov, Y. I. (2021). New atmospheric corrosion inhibitor of aluminum alloy D16. *Protection of Metals and Physical Chemistry of Surfaces, 57(7),* 1344–1351. https://doi.org/10.1134/S2070205121070170

76. Liu, C. D., Wu, M., Zhao, Z. H., Wang, X., Yang, Y. J. (2018). Study on the inhibition effect of chromate on stress corrosion of 2024 aluminum alloy in NaCl solution. *Nonferrous Metals Engineering, 8(1),* 61–65. https://doi.org/10.3969/j.issn.2095-1744.2018.01.013

77. Tan, Y. J., Liu, T. (2013). Inhibiting localized corrosion of aluminum and aluminum alloy by rare earth metal compounds: Behaviors and characteristics observed using an electrochemically integrated multi-electrode array. *Journal of the Electrochemical Society, 160(4),* C147–C158. https://doi.org/10.1149/2.068304jes

78. Tsai, S. T., Jean, C., Wen, C., Huang, L., Tsai, Y. et al. (2020). On the anti-corrosion property of dry-gel-conversion-grown MFI zeolite coating on aluminum alloy. *Materials, 13(20),* 1–14. https://doi.org/10.3390/ma13204595

79. Shruthi, T. K., Swain, G. M. (2018). Communication-role of trivalent chromium on the anti-corrosion properties of a TCP conversion coating on aluminum alloy 2024-T3. *Journal of the Electrochemical Society, 165(2),* C103–C105. https://doi.org/10.1149/2.1301802jes

80. Marshall, R., Kelly, R., Goff, A., Sprinkle, C. (2019). Galvanic corrosion between coated Al alloy plate and stainless steel fasteners: Part 1 FEM model development and validation. *Corrosion, 75(12),* 1461–1473. https://doi.org/10.5006/3308

81. Bastos, A. C., Karavai, O. V., Zheludkevich, M. L., Yasakau, K. A., Ferreira, M. G. S. (2010). Localised measurements of pH and dissolved oxygen as complements to SVET in the investigation of corrosion at defects in coated aluminum alloy. *Electroanalysis, 22(17),* 2009–2016. https://doi.org/10.1002/elan.201000076

82. Zhu, J. K., Li, S., Zhang, S. H., Wang, L. W., Yin, Z. J. et al. (2021). Research progress on solution strategy of "Corrosion-promotion behaviour" of graphene anticorrosion coatings. *Surface Technology, 50(10),* 14. https://doi.org/10.16490/j.cnki.issn.1001-3660.2021.10.011